

1 Planning of Distributed Energy Storage by A Complex Network Approach

2 Qigang Wu,¹ Fei Xue*² Shaofeng Lu,³ Lin Jiang,¹ Xiaoliang Wang,¹ and Tao Huang⁴

3 ^{1)Department of Electrical Engineering and Electronics, University of Liverpool, L69 3GL, Liverpool,}

4 UK

5 ^{2)Department of Electrical and Electronic Engineering, Xi'an Jiaotong-Liverpool University, 215123, Suzhou,}

6 China

7 ^{3)Shien-Ming Wu School of Intelligent Engineering, Guangzhou International Campus, South China University of Technology,}

8 Guangzhou, China

9 ^{4)Politecnico di Torino, Italy}

10 (*Electronic mail: Fei.Xue@xjtu.edu.cn)

11 (Dated: 22 March 2022)

12 Energy Storage System (ESS) has been considered one promising technology in dealing with challenges from the risk
 13 of power fluctuations and load mismatch in power grids. Distributed ESS (DESS) has better efficiency in reducing
 14 net losses and operating costs. The net-ability quantifies the power transmission ability across the grid where power
 15 is delivered from generators to loads under constraints. This paper proposes a new Complex Network-based metric:
 16 Energy Storage Performance (ESP), for assessing the significance of DESS inside a power grid. It aids the optimal
 17 location selections by improving grids' net-ability structurally. An auxiliary Genetic Algorithm (GA) sizing strategy
 18 is also deployed for deciding the optimal capacity of each DESS with the minimum daily operating and investment
 19 costs. The result shows that DESS improves the rate of cost reduction within an equivalent 24-hour daily operation.
 20 Moreover, this methodology finds quasi-optimal solutions with better feasibility and efficiency. The improvement of
 21 network performance by DESS depends on its original structure. The result shows that with the assistance of siting
 22 plan by complex network theory, the calculation efficiency improves and performs better in larger power grids. In the
 23 IEEE-30 test system, our solution is about 1/3 calculation time as the GA search. The quasi-optimal costs 1.8% more
 24 than the optimal searched by GA. Meanwhile, DESS can save more cost for networks with higher network-wide ESP
 25 value. In the IEEE-118 and IEEE-300 test systems, only the proposed hybrid-GA search can find a solution within a
 26 limited calculation time. Therefore, it could be promising in solving siting issues in the planning of smart grids.

27 I. INTRODUCTION

28 Due to the target of carbon emissions reduction and car-
 29 bon neutrality, Renewable Energy Source (RES) penetration
 30 is increasing rapidly in recent years¹. However, higher pen-
 31 etration of renewable energy will significantly increase the
 32 risk of power fluctuations and load mismatches, impacting
 33 power supply stability, reliability, and quality². Moreover,
 34 electrical power systems transfer progressively from central-
 35 ized control regimes to distributed control systems, increasing
 36 the complexity and uncertainty of power grids³. With mate-
 37 rials technology development, Energy Storage System (ESS)
 38 becomes a possible solution for solving these defects. ESS
 39 stores electrical energy and releases it later when needed with
 40 a suitable operating strategy⁴; therefore, it has been applied in
 41 several applications, particularly for electrified transportation
 42 and utility applications in power grids, such as load shifting,
 43 energy arbitrage and primary frequency regulation⁵. Mean-
 44 while, Distributed Energy Storage System (DESS) offers new
 45 solutions for power system planners. Compared with the con-
 46 ventional centralized ESS, DESS can deploy energy resources
 47 closer to users. For a large transmission or distribution system
 48 with more operational constraints and marginal losses, DESS
 49 has the potential to create more value locally. It supplies
 50 (or stores) energy at locations where the power transmission
 51 is frequently congested⁶. Paper⁷ discusses the impact of in-
 52 stalling DESS into a partitioned distribution network which
 53 can improve the degree of self-sufficient in each cluster.

54 However, the capacity of DESS is still constrained as the

55 energy and power density is limited due to modern materials
 56 and chemical technology. Meanwhile, the location of DESS
 57 in the utility network affects net losses due to the lossy trans-
 58 mission line and complex topological connections, which in-
 59 creases the operating cost for the grid operator. Thus, an opti-
 60 mal allocation for DESS is essential while applying it to power
 61 grid operation. Many research pieces optimize DESS alloca-
 62 tion to minimize its total cost inside the power grid, such as
 63 investment, operating, and equipment renewal costs^{8,9}. Some
 64 papers introduce optimization methods based on Optimal
 65 Power Flow (OPF) with storage installation, such as Stochas-
 66 tic Programming¹⁰, Mixed Integer Linear Programming¹¹,
 67 Genetic Algorithm (GA)¹² or Particle Swarm Optimization¹³.
 68 Yi *et al.*¹⁰ denotes a two-level optimization structure for al-
 69 locating DESSs and evaluating the dispatchability by MILP
 70 and benders decomposition. Similarly, article¹⁴ proposes a
 71 bi-level multi-objective optimization scheme for peak shav-
 72 ing and renewable energy compensation with the installation
 73 of DESS. Paper¹⁵ presents a near-optimal method for find-
 74 ing the minimum operating cost and daily storage investment
 75 under optimal location and sizing of DESSs by Unit Com-
 76 mitment. Ghofrani *et al.*¹⁶ introduces a framework for the
 77 optimal placement of DESS within a high wind penetrated
 78 power system. They applied a GA-enhanced, Hong's point
 79 estimation-based Probabilistic Optimal Power Flow (P-OPF)
 80 method to maximize wind power utilization over the schedul-
 81 ing period. Simulation results show that DESS have better uti-
 82 lization efficiency and reliability than centralized ESS. How-
 83 ever, due to the non-convex power flow constraints and the
 84 integer operating status of DESS, the determination of opti-

mal locations and capacities for DESSs is a non-deterministic polynomial-time (NP) hard problem, which is not efficient for an extensive system^{17,18}. Meanwhile, there is no direct metric for suggesting a proper amount of DESSs inside the power grid. Besides, no previous works were aware that DESSs might improve power grid performance to different extents due to various system structures and conditions. No metric has been introduced for assessing this difference as an inherent feature of different networks.

The Complex Network (CN) theory has been widely accepted as an impactful tool for analysing power grids' structural features. It has been developed to be a popular field as it connects disciplines, including graph theory, probability and statistics, statistical mechanics and control theory¹⁹. Many power network analysis applications are addressed with CN, such as assessment of robustness and vulnerability²⁰, power grid resilience and cascading failure analysis^{21,22}. Nevertheless, most of these research only consider the static topological aspects; structural approaches seldom discuss power flow dynamics and intra-hour relations inside the power network. DESS devices can operate under both charging and discharging modes, which is not considered a specific node type in previous works. The impact of DESS on power grids' performance and stability has not been evaluated from the structural perspective. To the best of our knowledge, no works have been done to apply Complex Networks in DESS planning. The contributions of this paper include:

- a). An index based on network topology analysis is introduced to evaluate the improvement of the network's performance when adding DESS on different buses.
- b). We argue that the performance improvement of power grids by DESS significantly depends on the original network structure.
- c). We propose that the number and sites of DESS-affiliated buses can be determined from a topological perspective. No paper has discussed how to decide the number of DESS-located buses by grid's topology and generator/(and load) setup.
- d). We use the metric above as part of DESSs optimal allocation, which accelerates the computational efficiency of GA search.

Section 2 introduces the concept of Energy Storage Performance (ESP) based on the idea of net-ability. Section 3 explains the optimization strategy for determining the optimal allocation of DESS. In section 4, simulation results are presented with a comparison between the pure heuristic algorithm and the proposed hybrid approach.

II. EVALUATION OF DESS PERFORMANCE BY STRUCTURE ANALYSIS

In this session, we propose a new metric, Energy Storage Performance (ESP), for assessing the significance of

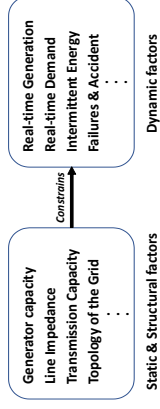


FIG. 1. Schematic of factors in power system operation. Static & Structural factors constrain the real-time operation of the power system.

equipped inside a specific power grid by the Complex Network work theory. Moreover, the optimal location can be determined by ranking the ESP of different buses as well.

As illustrated in Fig. 1, we classify two main groups of factors for assessing the real-world power system operations: Static & Structural and Dynamic factors. The static factors, such as the grid's topological connections or installed generator's capacity, are defined as permanently fixed parameters that cannot be changed during the whole power grid assessment procedure. It estimates the maximum ability to transfer power from generators to demands within the limitations of devices or transmission lines. On the other hand, the dynamic factors, including real-time load or quantity of intermittent energy in different periods, represent aspects that may change under different operating scenarios. Static factors constrain the network to operate within a reasonable domain, and dynamic factors determine how it works. However, with the integration of static and dynamic factors, the calculation complexity is expanded rapidly and inefficient for an extensive power network. Therefore, this paper will discuss a new metric that extracts static factors in power grids to evaluate transmission ability and efficiency improvement while integrating with DESS devices.

If a power grid is described as a graph, all buses, including generators, loads or substations, are considered as nodes. Transmission lines are also represented as weighted or unweighted edges connecting nodes. The overall performance of a Complex Network system is defined by global efficiency²³.

It measures the effectiveness of the information flow in both weighted and unweighted networks. Pagani *et al.*²⁴ denotes that the efficiency of transferring electricity is one aspect for measuring the power grid's goodness from the topological point of view. An improved metric, Net-ability, was designed to estimate the grid's performance²⁰. It quantifies the ability of power transmission across the whole grid where power is delivered concurrently from generators to loads under grid operational security. Considering a network $Y(V, L)$, V is the set of vertices which denote electric buses, and edges of the network, which symbolize power lines in the power grid, are represented as $L = \{(i, j)\} \subset V \times V$. From the electrical system perspective, functional node type distribution can be summarized as three types: Generator node $G = \{g_1, g_2, \dots, g_{|G|}\} \subset V$, Demand node $D = \{d_1, d_2, \dots, d_{|D|}\} \subset V$ for absorbing energy from generators, and transmission node $T = V - (G \cup D)$, an intermediate point for connecting edges without any gen-

eration or consumption of energy. The original Net-ability of Network Y was defined as²⁵:

$$N(Y) = \frac{1}{N_G N_D} \sum_{g \in G} \sum_{d \in D} \sum_{d \neq g} C_d^d \quad (1)$$

where N_G and N_D are the number of generator and load buses, Z_{gd}^d signifies the electrical distance between a generator-load pair $p(g, d) \in G \times D$. It implies the equivalent impedance between two nodes under the directionality of power flow²⁶ and is defined as:

$$Z_{gd}^d = \frac{U_g^d}{I_g} = z_{gg} - 2z_{gd} + z_{dd}, \quad (2)$$

where z_{gd} is the g^{th} -row, d^{th} -column element inside the impedance matrix of the power grid. Meanwhile, the equivalent topological transfer capability from generator node g to demand node d , C_g^d is described as following:

$$C_g^d = \min_{l \in L} \left(\frac{C_l^{cup}}{|f_l^{gd}|} \right), \quad (3)$$

where C_l^{cup} is the active power transmission capacity across the line l . f_l^{gd} is the Power Transfer Distribution Factor (PTDF)²⁷ of line l , which indicates variations of active power in transmission lines due to the unit active power injected in node g and extracted from node d . However, with the integration of DESS into the network, the DESS-located node cannot be defined only as a generator or load node since it has generator-load duality, which changes the node type distribution and resulting in mismatch for the Net-ability. If DESS is placed into a power grid, it becomes an intermediate point that temporarily stores the electricity from generator node(s) while charging mode and delivering power to load(s) under discharging mode. Additionally, it is supposed that charging and discharging cannot be operated simultaneously.

An electrical circuit schematic for power transmission through an alternative route across the DESS is shown in Fig. 2. The interconnection between a generation-load pair g and d is simplified as equivalent impedance Z_{eq} . If the DESS is not added into the grid, power is transmitted directly through this interconnection. The maximum transmitted power without any constraints for the generator in this transmission mode is equal to the equivalent transmission capacity described in Eq. (3). However, if the DESS is placed into the network, another route will be available for power flow. Power from the generator will be stored by DESS temporarily and released when necessary. To explore the impact of network structure on DESS performance, We assume that the generator-DESS pair's or DESS-load pair's transmission ability is constrained by the generator's or load's capacity and the topological transfer capability between the couple. The effect of the storage capacity itself is neglected in this stage. Therefore, the equivalent maximum transmission capacity from a generator g to a DESS bus e in charging mode P_{ge}^{max} is:

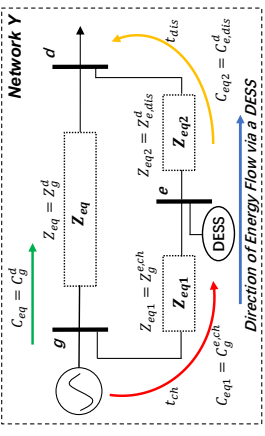


FIG. 2. Electrical circuit of system with DESS. Power transmission has an alternative route via DESS with extra *pseudo*-time consumption t_{ch} & t_{dis} .

$$P_{ge}^{max} = \min(C_g^{e, ch}, P_g^d), \quad (4)$$

$$C_g^{e, ch} = \min_{l \in L} \left(\frac{C_l^{cup}}{|f_l^{ge}|} \right).$$

Meanwhile, the equivalent impedance between generator bus g and DESS-located bus e while DESS in charging mode is:

$$Z_{ge}^{ch} = z_{gg} - 2z_{ge} + z_{ee}. \quad (5)$$

Similarly, the maximum transmitted power capacity between the DESS e and the demand d through the network is described as following:

$$P_{ed}^{max} = \min(C_e^{d, dis}, P_d), \quad (6)$$

$$C_e^{d, dis} = \min_{l \in L} \left(\frac{C_l^{cup}}{|f_l^{ed}|} \right).$$

The equivalent impedance between DESS bus e and load bus d is denoted as:

$$Z_{ed}^{dis} = z_{ee} - 2z_{ed} + z_{dd}. \quad (7)$$

As shown in Fig. 2, the equivalent impedance between g and d via DESS equals a series connection of Z_{ge}^{ch} and Z_{ed}^{dis} , which is denoted as:

$$Z_{gd}^d = Z_{ge}^{e, ch} + Z_{ed}^{d, dis}. \quad (8)$$

Here we propose a *Pseudo*-time of consumption in the DESS node to demonstrate the DESS *pseudo*-operation under the static CN analysis. It aims at clarifying the asynchronous of charging and discharging operations, which affects transmission efficiency. It is supposed that the quantity of shifted

energy required by a load bus d through a storage bus e is 279 evaluate a network's global capability for improving power
 284 Eng_{gd}^e and transmission losses are negligible. Besides, it is 280 transmission performance by DESS, which mainly depends
 285 assumed that transmission capabilities in the charging mode 281 on its static and structural characteristics, including the topo-
 286 in Eq. (4) and discharging mode in Eq. (6) are fully utilized. 282 logical connection of networks and the parameters of lines,
 287 Henceforward, the *pseudo*-time of consumption for the charge- 283 generators and loads, but not DESS itself. Meanwhile, as dis-
 288 ing and discharging processes are: 284 cussed in the previous paragraph, the *Net-ability* could also
 285 be described as energy transfer efficiency. The shifted elec-
 286 trical power between peak and off-peak periods can be trans-
 287 ferred more efficiently through DESSs. Thereby, we can re-
 288 veal the effectiveness of installing DESS in the network by
 289 the structural analysis. ESP_G can also compare DESS pro-
 290 ductivity among different networks without time-consuming
 291 optimal allocation.

$$\begin{aligned}
 t_{ch} &= \frac{Eng_{gd}^e}{P_{ge}^{\max}}, \\
 t_{dis} &= \frac{Eng_{gd}^e}{P_{ed}^{\max}}.
 \end{aligned} \tag{9}$$

289 While the DESS is operating, the *pseudo*-time of consump-
 290 tion can be summed, as the delivered energy from a generator
 291 to DESS and from DESS to the load are identical. Thus, the 292
 293 equivalent transmission capability through DESS from g to d
 294 is:

$$P_{ge}^{pd} = \frac{Eng_{gd}^e}{t_{ch} + t_{dis}} = \frac{P_{ge}^{\max} \cdot P_{ed}^{\max}}{P_{ge}^{\max} + P_{ed}^{\max}}.$$

284 From Eq. (10), the equivalent capacity is irrelevant to the
 285 quantity of dispatched energy Eng_{gd}^e . Referring to the defini-
 286 tion of net-ability, we then introduce a metric Energy Storage
 287 Performance (ESP) for assessing the improvement of network
 288 efficiency by installing DESSs. The nodal Energy Storage
 289 Performance (ESP_n) for bus e is defined as:

$$ESP_n(e) = \frac{1}{N_G N_D} \sum_{\substack{g \in G \\ d \in D}} P_{gd}^{pd},$$

290 where $P = \{(g, d)\} = G \times D$ is the notation of all generator-
 291 load pairs. For a particular generator-load pair p , if a DESS is 311
 292 located on either load or generator buses, power will be trans- 312
 293 mitted directly between g or d and e . The power transmission 313
 294 between overlapped nodes is not through the network; there- 314
 295 fore, it is not discussed in evaluating network features. 315
 296 Afterwards, we can calculate the ESP_n for every node and 316
 297 rank these data for determining the priority of buses placing 317
 298 DESSs. It will accelerate the calculation procedure of DESS 318
 299 optimal capacities and locations allocation as it decides loca- 319
 290 tions in advance, reducing variables in the NP-hard allocation 320
 291 problem. 321
 292 Moreover, the global network-wide Energy Storage Perfor- 322
 293 mance (ESP_G) of the grid $Y(V, L)$ is defined as an average 323
 294 value over all buses in the entire network: 324

$$ESP_G(Y) = \frac{1}{N_V} \sum_{e \in V} ESP_n(e), \tag{12}$$

295 where V is the set of all buses inside network Y , and N_V is 327
 296 the number of buses inside the grid. The ESP_G is equivalent 328
 297 to an additive Net-ability value, where it provides an alterna- 329
 298 tive route for power flow through DESS(s). This index can 330
 299 DESSs. The objective function can be summarized as:

III. OPTIMAL ALLOCATION STRATEGY OF DESS

293 The installation of DESS should improve power transmis-
 294 sion efficiency by adjusting the spatial and temporal distribu-
 295 tion of power flow. The ESP metric considers DESS's spatial
 296 contribution to offer a new route for power transmission be-
 297 tween any generator-load pair through DESS. It avoids possi-
 298 ble congestions in a power grid and improves the stability of
 299 the power grid. However, in an actual engineering application,
 300 the sizing of DESS is also critical because of the trade-off be-
 301 tween operating costs from generators and DESS investment
 302 costs.

303 Fig. 3 illustrates the framework of optimal allocation strat-
 304 egy for DESS assigned in this paper. DESS has three operat-
 305 ing states: Charge, Discharge and Idle. It can be expressed as
 306 a group of integers. Meanwhile, the DESS's capacity is not
 307 continuous in engineering applications. The AC power flow
 308 is non-linear as well, which decides the actual power varia-
 309 tion for DESSs. Therefore, the optimal allocation of DESS is
 310 a mixed-integer non-linear problem. For this reason, we select
 311 the GA as the main optimization tool. GA has good reliabil-
 312 ity during the calculation procedure. It can easily collaborate
 313 with existing models or integrate into hybrid approaches as
 314 well^{28,29}. Meanwhile, the function can be easily transformed
 315 into the parallel implementation without restrictions on the
 316 program they process. However, GA is a random search meta-
 317 heuristic algorithm. If the number of variables is not limited,
 318 larger population sizes are necessary, which causes the itera-
 319 tions to be very slow. Henceforward, the decision is decom-
 320 posed into a two-step model for reducing the complexity of
 321 the decision. Firstly, the numbers of DESS-integrated buses
 322 and their locations are selected by $ESP_n(e)$ in descending or-
 323 der. Afterwards, the size of each DESSs is determined by a
 324 hierarchical optimization model indicated in this section.

A. Optimal sizing of DESS

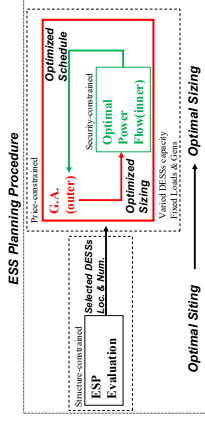


FIG. 3. Framework of optimal allocation of DESS. ESP evaluation determines DESS number & location, and the capacity is subsequently allocated by hierarchical GA search.

$$f_{\text{obj.}} = \min \left\{ \underbrace{\sum_x \sum_s^{f_s^c} \cdot \sum_{k=24}^{f_{\text{oper.}}[k]} + \sum_{i \in \mathcal{E}} C_{0n}^{\text{inv}}}_{\text{operating cost}} \right\}, \quad (13)$$

DESS inv. cost

where \mathcal{E} is the set of installed DESSs variables, including DESS's location and capacity. $f_{\text{oper.}}$ represents the operating cost of devices during a single time interval. f_s^c indicates the weight function for different load scenarios. The investment cost of DESS is C_{0n}^{inv} . The objective function is a summation of the operating cost from generators, the replacement cost and the investment cost from DESSs. We propose a bi-level hierarchical optimization model for determining the optimal sizing problem as it combines the consideration of economic and technical issues. The outer optimization model selects DESS capacity commitments by minimizing the sum of DESSs investment cost and the 24-hour total operating cost from generator and DESSs. The inner layer optimization is designed for minimizing the total operating cost from all generators and DESSs within a specific period by adjusting the active power output of all dispatchable generators and DESS operations. The variables in this stage are active power outputs of dispatchable generators, and DESSs operating states and power. Besides, the capacity of DESS is deterministic in this stage. The result of the inner optimization layer represents the optimized operating schedule for generators and DESS under a particular combination of DESSs allocations. In this paper, we choose multi-period AC-OPF as the inner optimization method and GA as the outer optimization tool.

1. Outer optimization for DESS operation based on Genetic Algorithm

This section introduces the tool for searching the optimal result of the objective function discussed before. The outer layer includes a selection method for the DESS capacity. Genetic Algorithm is emerging as an efficient optimization method widely used to solve the non-linear, non-convex and mixed-integer DESS placement¹⁶. This stage's primary work encodes the DESS optimal sizing problem into GA's chromosomes and defines the fitness function. The variable is equivalent to the remaining energy level in the preceding interval; therefore,

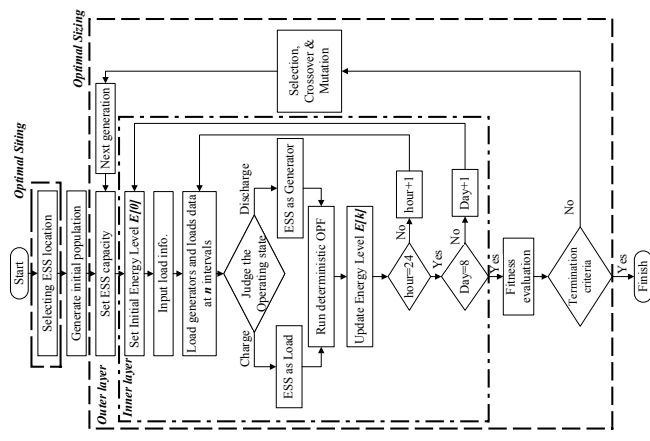


FIG. 4. The overall structure of optimal allocation of DESS.

alent to a gene, and it constitutes chromosomes. In the presented work, the fitness function is denoted as in Eq. (13). The overall algorithm structure of the optimal allocation of DESS is presented in Fig. 4. Firstly, the optimal position is decided by the structural analysis methodology noticed in the previous section. Then, the initial population in GA is generated with random DESS(s) capacity. For every population generated by GA, inner optimizations are calculated to evaluate each individual's fitness function. Meanwhile, the actual discharge or charge power of DESSs are determined by inner OPF and the energy level for DESSs is updated simultaneously.

2. Inner optimization for DESS operation based on OPF

We propose AC-OPF as the optimization strategy in the inner layer. The internal optimization is to calculate the operating cost for the fitness function of the outer layer. First, a daily load levelling factor for all load buses is selected. The optimization output for each generator, including DESS, is calculated by the deterministic AC-OPF, subsequently. The charging or discharging of DESS in each interval depends on the remaining energy level in the preceding interval; therefore,

energy stored in the DESS is updated from the result simulta-
 neously. The progress is repeated for 24 hours, and the daily
 operating cost is assessed by summing the fuel cost within 24
 hours. Afterwards, this process will be repeated eight times
 to demonstrate eight scenarios where simulate the cost under
 weekdays or weekends in four seasons. For the deterministic
 AC optimal power flow, the objective function is:

$$\begin{aligned}
 f_{obj}^{inner} &= \min \{f_{oper}\} = \min_{P,Q,V,\theta} \left\{ \sum_{g \in G} f_g(E_g) + \sum_{n \in E} f_{rep}(E_n) \right\} \\
 &= \min \left\{ \sum_{g \in G} (a_g P_g^2 + b_g P_g + c_g) + \sum_{n \in E} (a_n \cdot P_n^{DESS}) \right\} \\
 &= \min \left\{ \sum_{g \in G} (a_g P_g^2 + b_g P_g + c_g) + \sum_{n \in E} \frac{1}{IC} \frac{Co_{rep} \cdot E_n}{\Delta t} \cdot P_n^{DESS} \right\}, \quad (14)
 \end{aligned}$$

where a_g , b_g and c_g are the operating cost polynomial coeffi-
 cient for generator g , respectively. P_n^{DESS} is the power input
 (or output) of DESS in charge (or discharge) mode. We sup-
 pose that the replacement cost of DESS is part of the operat-
 ing cost and is spread out into per unit of DESS charge (and
 discharge) energy. Co_{rep} is the capital replacement cost for a
 piece of DESS equipment, and the life cycle for this particular
 device is represented as LC . This function is subject to:

Equality constraints:

$$P_i = P_{gi} - P_{li} = \sum_{k=1}^{N_{bus}} V_i V_k [G_{ik} \cos \theta_{ik} + B_{ik} \sin \theta_{ik}], \quad (15)$$

$$Q_i = Q_{gi} - Q_{li} = \sum_{k=1}^{N_{bus}} V_i V_k [G_{ik} \sin \theta_{ik} + B_{ik} \cos \theta_{ik}].$$

Inequality constraints:

$$V_i^{\min} \leq |V_i| \leq V_i^{\max},$$

$$S_i \leq S_i^{\max},$$

$$P_{gi}^{\min} \leq P_{gi} \leq P_{gi}^{\max},$$

$$Q_{gi}^{\min} \leq Q_{gi} \leq Q_{gi}^{\max}$$

The equality constraints Eq. (15) represent the active and
 reactive power balancing for all nodes i in each time interval
 t . We assume that DESS shifts active power from generators
 only without consuming or storing reactive power. The limi-
 tation for nodal voltage margin is described in Eq. (16). Line
 capacity for power flow is presented in Eq. (17). Equation
 (18) indicates active and reactive power generation limits for
 all generators.

The AC-OPF program can optimize the output of active
 and reactive power of each energy source individually, in-
 cluding generators and DESS in charge (as dispatchable load)
 or discharge (as generator) mode. In this paper, we suppose

TABLE I. Weight of load-leveling in different scenarios.

	S1	S2	S3	S4	S5	S6	S7	S8
Season	Spring	Spring	Summer	Summer	Autumn	Autumn	Winter	Winter
Day-type	Wkd	Wkd	Wkd	Wkd	Wkd	Wkd	Wkd	Wkd
f_s^{sc}	5/28	2/28	5/28	2/28	5/28	2/28	5/28	2/28

that DESS do not participate in adjusting the reactive power;
 the balance of reactive power is supplied by generators only.
 Meanwhile, power output or input by DESS is limited by con-
 straints of charging and discharging power and stored energy
 level as well. The AC-OPF is implemented by an open-source
 MATLAB-based simulation package, MATPOWER³⁰.

B. System description

For verifying the validity of the ESP metric, a power system
 integrated with DESS devices is modelled in this section. The
 fluctuation of demands within 24 hours is considered in this
 model.

1. Load levelling factor modelling

The random model of loads inside the system is character-
 ized as the Gaussian distribution with upper limits LR_{up} and
 lower limits LR_{lo} ^{16,31}:

$$f_{LR}(lr) = \begin{cases} \frac{1}{\sqrt{2\pi\sigma^2}} \exp\left[-\frac{(lr-\mu)^2}{2\sigma^2}\right], & LR_{lo} \leq lr \leq LR_{up}, \\ 0, & lr < LR_{lo}, lr > LR_{up} \end{cases}, \quad (19)$$

where lr represents the hourly demand levelling within target
 periods. Estimation of μ and σ values are based on the IEEE-
 RTS³² system, which provides hourly, daily and seasonally
 peak load in the percentage of nominal demands. Besides, the
 load curves on weekdays and weekends are different. We se-
 lect eight 24-hour load-level scenarios under the varied weight
 f_s^{sc} in varied seasons and day types as listed in Table I. In each
 scenario, a 24-hour load levelling factor is calculated for all
 load buses from Eq. (19).

2. Modelling of DESS

The purpose of DESS installation in this paper is for shift-
 ing the excess electric energy generated from generators into
 peak demand hours; otherwise, it will be mismatched, and
 the system cannot operate properly. The instantaneous energy
 balance in the DESS is discretized and described as:

$$E_n[k] = E_n[k-1] + (\alpha \cdot \eta_c^k P_{n,c}[k] - \beta \cdot \frac{P_{n,d}[k]}{\eta_d^k}) \cdot \Delta t, \quad (20)$$

446 where $E_n[k]$ is the energy stored in the n^{th} DESS unit at k^{th} 474 **IV. CASE STUDY**

447 time interval, $E_n[k-1]$ represents the energy at the last inter-
 448 val, similarly, η_n^c and η_n^d are energy conversion coefficient 475
 449 in charge and discharge mode, respectively. α and β are 476
 450 the DESS charging or discharging status. Also, we suppose 477
 451 that the charging power $P_{n,c}[k]$ and discharging power $P_{n,d}[k]$ 478
 452 are constant during the time interval. Due to limitations of 479
 453 DESS's physical characteristics, the operation of the unit is 480
 454 constrained to: 481

$$482 \text{SoC}_n^{\min} \leq \text{SoC}_n[k] \leq \text{SoC}_n^{\max}, \quad (21) 484$$

485 where $\text{SoC}_n[k]$ is the State-of-Charge for DESS at k^{th} interval
 486 as following:

$$487 E_n[k] = \text{SoC}_n[k] \cdot E_n. \quad (22) 489$$

487 Based on the constraint of energy level, the peak charging 488
 488 and discharging power within the interval k are constrained to: 489

$$490 0 \leq P_{n,c}[k] \leq \min(P_{n,c}^{\max}, \frac{E_n \cdot \text{SoC}_n^{\max} - E_n[k-1]}{\eta_n^c}),$$

$$491 0 \leq P_{n,d}[k] \leq \min(P_{n,d}^{\max}, (E_n[k-1] - E_n \cdot \text{SoC}_n^{\min}) \cdot \eta_n^d), \quad (23) 496$$

495 where the energy level at the end of each interval cannot ex- 498
 496 ceed its limitations. 499

497 Our objective function is to minimize the equivalent 24-
 498 hour daily cost, including ESSs capital cost, operating, and
 499 fuel costs from existing generators. Therefore, an economic 501
 500 analysis is established for integrating these costs. The energy 502
 501 capacity constraints DESS charge and discharge rate; thus, the
 502 apportioned daily installation investment cost of a DESS is: 503

$$504 C_{o_{\text{inv}}}^{\text{inv}} = k_{\text{inv}}^{\text{RR}} \cdot C_{o_{\text{inv}}}^{\text{cap}} \cdot E_n \quad (24) 506$$

507 where $C_{o_{\text{inv}}}^{\text{cap}}$ is the capital investment cost for the DESS. The 508
 508 capital cost factor $k_{\text{inv}}^{\text{RR}}$ is defined by using the Internal Rate of
 509 Return:

$$510 k_{\text{inv}}^{\text{RR}} = \frac{1}{365} \frac{r_n(1+r_n)^y}{(1+r_n)^{y+1} - 1}, \quad (25) 512$$

513 where r_n represents the interest rate, and y is the depreciation 514
 514 period. The primary purpose for DESS is time-shift the ex- 515
 515 cess electric energy from generators into peak demand period; 517
 516 therefore, the operating criteria is modelled as below: 518

$$519 \alpha = 0, \beta = 1, \quad \text{Discharge state.} 521$$

$$520 \alpha = 1, \beta = 0, \quad \text{Charge state.} 522$$

In this section, the proposed optimal allocation strategy of
 DESS is tested on the IEEE-30 system under five cases to val-
 idate the ESP metric's effectiveness. The proposed ESP-GA
 hybrid method and the pure GA optimal allocation algorithm
 are compared in terms of calculation speed and accuracy. Sub-
 section B simulates the multi-DESSs optimal allocation strat-
 egy proposed in this paper for the IEEE 30-bus, 118-bus and
 300-bus systems. MATPOWER is applied as the optimiza-
 tion tool for the inner OPF calculation, and MATLAB Global
 Optimization Toolbox implements the GA.

A. Evaluation of DESS in the IEEE-30 bus system under different circumstances

1. Description of test scenarios in IEEE-30 system

We distinguished the power grid operation factors into two
 parts: static and dynamic factors. The ESP is for measuring
 the effect from static factors. Therefore, we validate the ESP
 by discussing impacts from three static elements in the given
 IEEE-30 system in this part: 1. Distributions of generator ca-
 pacity P_g ; 2. Transmission capacity in different lines $C_{i,\text{Case}}$ in
 the topological connection in the power grid. More-
 over, the hourly load-leveling, which belongs to dynamic fac-
 tors, is also discussed in this test. Therefore, we design five
 scenarios by modifying the original IEEE-30 bus system and
 comparing the difference between them afterward. The sum-
 mary of each case is listed as below:

- I. Original IEEE-30 bus system.
- II. Modifying each generator's capacity. The allocated ca-
 pacities for each generator are identical.
- III. Limiting maximum capacity for lines.
- IV. Modifying the grid's structure. Three lines are re-
 moved, and four lines are installed.
- V. Changing hourly load leveling in all nodes for every
 tested hour.

Table II enumerates the configuration for the testing system
 and differences in cases. Detailed modifications of Case III
 and Case IV are attached in Table III and Fig. 5. We suppose
 that the transmission line is "ideal" in case III. Modifications
 for line capacity cannot lead to changes in its impedance. For
 Case V, a new set of load-leveling data is generated by Eq.
 (19) with an updated hourly peak total demand to 269.82 MW.
 The numbers of generators, total generation capacity, and total
 demand within every 24 hours in eight typical days are static
 in all cases. The DESS planning in all five cases is performed
 by both the ESP-GA hybrid and pure GA methods. If there
 are no limitations for the DESS number, the pure GA method
 tends to allocate DESS on every bus. This is undoubtedly
 beneficial for system operation in theory, but it is not feasi-
 ble in practical engineering. Therefore, in all five cases, both

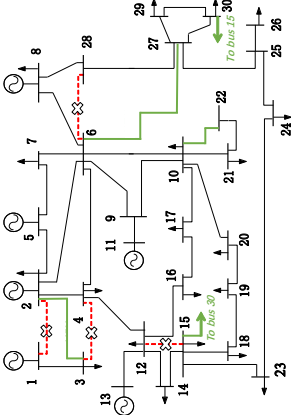


FIG. 5. Schematic for the IEEE-30 test system. Dashed red lines (removed) and solid green lines (added) are modifications in Case IV. A transmission line between bus 15 and bus 30 is added in Case IV.

TABLE II. Configuration for IEEE-30. N_{DESS} , N_{gen} and M_{branch} is the number of DESS, generators and branches inside the IEEE-30 test system, respectively. The net demand in case V increases as the distribution of load-levelling in different buses changes.

	N_{DESS}	N_{gen}	N_{branch}	$\sum P_{gen,max}[k]$	$\sum P_{load,max}[k]$
3	6	41	250.0 MW	269.8 MW (Case V)	265.7 MW (Others)

523 methods consider the allocation of three DESS devices. Each
 524 DESS device is possibly installed from bus 1 to bus 30.

525 2. Results and discussions for five cases

526 Firstly, table IV introduces the nodal ESP and network-
 527 wide ESP values in five testing cases. In Case V, the hourly
 528 load levelling factor is modified only, and there are no changes
 529 in the grid's topological connection, generator capacity & lo-
 530 cation and demand levelling; therefore, it has the same ESP_n
 531 performance as Case I. The performance in Case III is sim-
 532 ilar to Case I as well. The limitation constrains less power
 533 flow from transmission lines. With the modification for allo-
 534 cations of generators' capacity, Case II achieves the best ESP_n
 535 score as the distribution of generation is more balanced than
 536 the original case. Fig. 6 illustrates the value of ESP_n in two
 537 selected cases: Case I and Case IV. Bars with red colour rep-
 538 resent the pre-selected buses where DESSs will be located in
 539 further analysis. Initially, in bus 1, two lines are connected
 540 with the affiliation of a generator with the largest capacity.
 541 The nodal performance ESP_n in bus 1 can achieve a higher
 542 rank in Case I. However, with the modification of lines con-
 543 nection, the number of lines to bus 1 is reduced to one. There-
 544 fore, the increase in electrical distance between bus 1 and
 545 other generation buses and load buses eventually cuts trans-
 546 mission efficiency. As a result, the value of ESP_n falls in Case
 547 IV because of higher losses of power transmission between
 548 bus 1 and other buses compared with Case I. Conversely, for

TABLE III. Configuration for case III modification. Line's capacity in case III is limited individually.

Branch No.	$C_{l,Case III}^{cap}$ (MW)	$C_{l,orig}^{cap}$ (MW)
1, 2, 4, 5, 9	130	
7	90	
8	70	973
3, 6, 11, 13, 14, 15, 16, 36	65	
10, 12, 17, 18, 19, 24, 25,	32	
26, 27, 28, 29, 40, 41	16	
OTHERs		

TABLE IV. ESP result in the IEEE-30 system. $ESP_n(e)$ rank shows the descending order of value of nodal ESP_n .

Case	Modification	$ESP_n^*(V)$	$ESP_n(e)$ Rank	$ESP_{n,max}$
I	None	25.42	2,1,8,4	87.66
II	Generator Capacity	31.37	2,1,8,5	103.1
III	Line Capacity	25.05	2,1,8,4	86.42
IV	Line Connection	23.57	2,5,8,4	70.31
V	Load Levelling	25.42	2,1,8,4	87.66

549 some nodes, e.g., bus 27 and bus 30, connecting more lines
 550 leads to a reduction in electrical distances, which results in
 551 better score of ESP_n . The detailed settings of DESS are listed
 552 in Table V. The only difference between DESSs is its installed
 553 capacity. Other parameters, such as the charging or discharg-
 554 ing efficiency, are the same. The operation strategy of DESS
 555 is for peak-shaving, where it discharges when the generation
 556 is insufficient within an interval and charges or idle in remain-
 557 ing periods. Table VI shows the result of DESS allocated lo-
 558 cations and capacities using the hybrid ESP-GA method and
 559 pure GA method. For example, in Case I, two DESSs are lo-
 560 cated in bus 1 by GA-only algorithm with the capacity of 20
 561 MWh and 8 MWh, respectively. Overall, all factors, includ-
 562 ing the structural, static and dynamic factors discussed in this
 563 case, could affect the 24-hour total costs. The balanced gen-
 564 erator distribution stated in Case II shows the best economic
 565 efficiency in all cases and minimum DESS installation. More-
 566 over, modifications in the static factors tested in Case II and
 567 Case IV can affect the results. The most significant devia-
 568 tion of daily cost and installed capacities of DESS occurred in
 569 Case IV. The correctness of pre-defined location by ESP met-
 570 ric is acceptable as well. Bus 2 inside the IEEE-30 bus sys-
 571 tem receives the highest nodal ESP values in all five cases,
 572 and more DESS capacities are allocated on this bus.

573 The result in Table VI proves that the cost-efficiency of
 574 the entire network operation is increased with higher value
 575 of ESP_n . The ESP metric is developed from the concept of
 576 Complex Network efficiency and net-ability. It represents the
 577 power grid's performance and energy transfer efficiency mea-
 578 sured by Complex Network Theory. Thus, higher ESP_n im-
 579 proves the energy delivery productivity with the integration of
 580 the DESS system.

581 Finally, as illustrated in fig. 4, DESS optimal allocation cal-
 582 culation steps are similar between the hybrid ESP-GA and the
 583 pure GA search. Therefore, we compare the converged gen-

TABLE V. Parameters for DESS configuration used in this paper.

SoC ^{max}	η_{in}^d	LC/cycles	$C_{0,inv}^{cap}$ (\$/MWh)	y/hrs
0.9	90%	1000	53000	20
SoC ^{min}	η_{in}^c	Min. Units	$C_{0,rep}^{cap}$ (\$/MWh)	r_p
0.1	95%	1MWh	40000	10 %

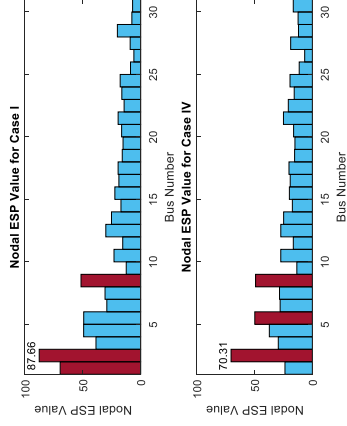


FIG. 6. The nodal ESP value in case I & IV. Highlighted red bars represent better ESP value in these buses and are selected as DESS-installed locations.

eration as proof of calculation efficiency. The 7th column represents the converged generations in GA, which displays the calculation efficiency between the conventional GA and ESP-GA hybrid methods. The calculation efficiency is improved with less growth in the 24-hour total costs between ESP-GA hybrid searching and the pure GA method for every case. The most considerable cost sacrifice occurs in Case V, with a loss of 1.80%. In conclusion, the CN-based ESP solution can accelerate the calculation time by per-defining the location of DESS. Meanwhile, DESS has better performance and saves more cost for networks with higher network-wide ESP.

B. DESS allocation in different systems

In this part, the effectiveness of network-wide ESP metric and the calculation efficiency of DESS allocation are discussed between ESP-GA hybrid searching method and GA-only for the IEEE 30-bus, 118-bus and 300-bus testing systems. Table VII and Fig. 7 illustrate the value of nodal ESP in different systems. The first column represents the selection criterion for buses to install DESS (levelling ratio of maximum nodal ESP values in the tested system). The allocation strategy for DESS with the simultaneous analysis for optimal locations and capacities is an NP-hard problem. The computation complexity is increased rapidly with the increment of system scale. Therefore, we make a trade-off between the computation efficiency and global accuracy for the

TABLE VI. Results of Tested System. Numbers inside the brackets mean that these DESSs are located inside the same bus, and they could be merged as a single unit in later analysis.

Cases	Method	Locat.	Capa.	Total ESP_p	Con. Gen	Gen Cost (10^5)	
I	Hybrid	2,1,8	18,3,54	75	25,42	31	2,04
	GA	3,(1,1)	48,(20,8)	76	25,42	94	2,03
II	Hybrid	2,1,8	5,10,43	58	31,39	33	1,96
	GA	(1,1),2	(17,23),19	59	31,39	91	1,95
III	Hybrid	2,1,8	17,4,54	74	25,05	36	2,04
	GA	(1,1),2	(13,30),34	77	25,05	71	2,02
IV	Hybrid	2,5,8	1,40,83	124	23,57	28	2,23
	GA	5,(4,4)	88,(17,18)	123	23,57	116	2,22
V	Hybrid	2,1,8	70,12,5	87	25,42	30	2,20
	GA	2,(1,1)	80,(1,1)	82	25,42	103	2,16

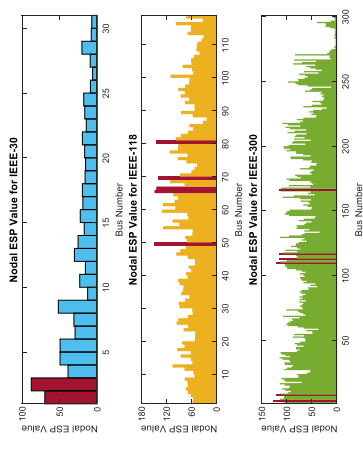


FIG. 7. The Nodal ESP Value in Case 30, 118 & 300. Highlighted red bars represent better ESP value in these buses and are selected as DESS-installed locations.

optimal allocation strategy of DESSs in the following analysis. The number of installed DESS is decided where the nodal ESP value in its locations is over 90% of the maximum ESP value, as indicated by the first column of Table VII. For example, in 300-bus system, the value of ESP_p in bus 133 is 114,78, where it is 90,19% of ESP_p in bus 3 ($ESP_p = 126,6$).

Henceforward, the number of DESSs installed in the 30-bus, 118-bus and 300-bus systems is 3, 5 and 6, respectively. The summary of network configurations in three cases is listed in Table VIII. DESS charging and discharging coefficient is the same as Table V. The population size, mutation rate, and other GA settings are the same in both ESP-GA hybrid and pure GA methods. Table IX reveals the numerical results of the DESS allocations for two methods. It is clear that with the increasing number of DESS installed locations, more generations in GA search are required in both ESP-GA hybrid and GA searching methods. The maximum number of generations of both methods is set as 150. In the IEEE-118 and IEEE-300 test systems, the pure GA searching method cannot find solutions within the maximum generation numbers. For a single 24-hour AC-OPP inner-layer optimization, more time is

TABLE VII. Ranking of Nodal ESP in Different Cases. The first column means the percentile of nodal ESP value. For example, 4 buses (bus No. 49, 65, 66,80) have better ESP_n value in the 95th percentile.

%	IEEE-30	IEEE-118	IEEE-300
>95	2	49,65,66,80	3,7,130
>90	2	49,65,66,80,69	3,7,130,137,187,133
>85	2	(11 buses)	(22 buses)
>80	2	(20 buses)	(42 buses)
>75	2,1	(29 buses)	(59 buses)

TABLE VIII. Overall configuration and network-wide ESP value of IEEE-30, IEEE-118 and IEEE-300 bus system.

Sys.	$\sum P_{gen,max}[k]$	$\sum P_{load,max}[k]$	$ESP_n(Y)$
30	250.00	265.67	25.42
118	3592.3	3987.8	75.56
300	21786	22569	67.06

consumed by increasing case size. With assistance from ESP pre-defined locations, the search space is limited, resulting in a rapid acceleration of calculation procedure with appropriate sacrifice in calculation accuracy. A set of quasi-optimal results could be found in a more extensive system restricting calculation times.

C. Discussion of ESP-GA hybrid method

In the previous section, we have focused on applying the ESP metric for DESS allocation under different cases. The hybrid ESP-GA search can split the DESS allocation into two individual sub-problems and perform well in a large-scale system. This part will discuss the calculation efficiency of the ESP-GA method. Meanwhile, we evaluate the cost performance of the ESP-GA method by comparing the cost between different DESS locations sorted by the nodal ESP value. The program is run at Intel Core i5-6500 quad-core@3.2GHz, 8G RAM and MATLAB 2018b.

Table X records the computation time of ESP_n and GA search. Referring to the flow chart of DESS allocation strategy in fig. 4, pure GA search and hybrid GA-ESP have similar structures at the stage of optimal cost evaluation. GA-ESP has fewer variables as it determines the location of DESS in advance, leading to a reduction in computation duty than pure GA search. For example, in the 30-bus system, the ESP_n value calculation time, which decides the preferred location of DESS, is 0.544s. The calculation time for GA search is up to 666.61s. Table IX shows that the hybrid GA search has 63 fewer converged generations than the pure GA search. With a quick DESS location evaluation iteration, ESP-GA search significantly reduces the calculating time.

Table XI shows the cost efficiency of DESS allocation in different locations. We sorted the nodal ESP value in ascending order and selected the same number of buses as the “best”

TABLE IX. Result of DESS rating in IEEE-30, 118, & 300 bus system. Numbers inside the brackets mean that these DESSs are located inside the same bus, and they could be merged as a single unit in later analysis. The pure GA algorithm is not converged in IEEE-118 and IEEE-300 bus system within preset max. generations.

Sys.	Method	Locat.	Capa.	Total ESP_n	Con. Gen	Cost (10^5)
30	Hybrid	2,1,8	18,3,54	75	25,42	31
	GA	3, (1,1)	48,(20,8)	76	25,42	94
118	Hybrid	49,65,66, 80,69	157,170,73, 178,8	1043	75,56	88
	GA		N/A (Exceed max. generation)			
300	Hybrid	3,7,130, 137,187,133	283,31,54, 317,105,190,3	2973	67,07	147
	GA		N/A (Exceed max. generation)			83.6

TABLE X. Computing time of ESP_n and GA in IEEE-30, IEEE-118 & IEEE-300 case. The 3rd column records the averaged time consumption in the GA search method per generation. The computer specification is Core i5-6500 4-core@3.2GHz, 8G RAM, MATLAB 2018b. Unit in this table is second.

Sys.	ESP_n (s)	GA/gen.(s)
30	0.544	666.61
118	465.23	1480.9
300	21086	7699.2

case displayed in Table IX, where is named as “worst” case listed in 2nd column. The result indicates that in all cases, including IEEE-30 under different modifications, IEEE-118 and IEEE-300 test system, the total cost increases while DESSs located in nodes with less ESP_n values. As the operating states, such as generator distribution and hourly load, are the same inside one targeted test case, DESS has a worse ability for adjusting the quantity of power flow between generator-load pairs, resulting in more power losses during the mission. Meanwhile, a more significant gap of ESP value leads to more increment of the total cost. For example, the ratio of total ESP_n between the best and the worst scenario shows that there is the most significant difference in the 300-bus system. Referring to the 300-bus system schematic³³, selected nodes with the least value of ESP_n are located at the sub-distribution-network with a Point of Common Coupling (PCC) at bus 39. Interactions between nodes chosen and the main grid, including the quantity of power exchange and the equivalent line impedance, are worse than nodes designated by the better ESP_n value. Moreover, the installed capacity of DESS in the worst condition can also prove that the choice of location is not appropriate. The total capacity of DESS is 18 MWh, which is much smaller than its networkwide generation and demand. DESSs in these nodes are not very involved in adjusting the power flow distribution. The redundant capacity of DESS in an improper position increases the total cost only, without any hourly operating cost improvement, and is optimized by GA afterwards. In conclusion, the DESS performance efficiency can be evaluated quickly by sorting the value of nodal ESP.

TABLE XI. Result of DESS allocation in IEEE-30, 118, & 300 bus system with different pre-defined locations. The searching method of all cases is by the ESP-GA hybrid search. We select nodes with ESP_n value in ascending and descending order as the "Best cond." and "Worst cond.". The 5th column represents the total value of nodal ESP_n value. The ratio between the highest and lowest total ESP values is recorded in 7th column. In the last column, it represents the percentage of cost increment than the best scenario.

Case	Cond.	Locat.	DESS Cap.	$\sum ESP_n$	cost(10^5)	B/W $\sum ESP_n$	Cost. Inc.
I	Best	2,1,8	18,3,54	208.75	2.04	10.28	10.54%
	Worst	26,30,29	20,32,20	20.32	2.26		
II	Best	2,1,8	5,10,43	251.22	1.96	9.96	10.20%
	Worst	26,30,29	15,26,15	25.22	2.16		
30	Best	2,1,8	17,4,54	205.93	2.04	11.66	10.78%
	Worst	26,30,29	20,31,20	17.65	2.26		
IV	Best	2,5,8	1,40,83	169.21	2.23	5.63	8.24%
	Worst	26,25,28	4,90,28	30.03	2.41		
V	Best	2,1,8	70,12,5	208.75	2.20	10.28	4.41%
	Worst	26,30,29	29,23,24	20.32	2.30		
IEEE-118	Best	49,65,66, 80,69	157,170,73, 178,8	726.61	17.20	4.67	2.83%
	Worst	87,112,86, 117,111	4,63,7,3,32	155.72	17.69		
IEEE-300	Best	3,7,130	283,311,54, 137,187,133	712.90	83.61	61.65	27.51%
	Worst	9042,9025,9026 9032,9033,9031	317,105,1903 5,2,5,3,1,2	11.56	106.6		

V. CONCLUSIONS

work theory could contribute much more in planning smart grids by solving siting issues.

A network-structure-analysis based methodology for optimal siting of Distributed ESS is presented in this paper. It provides a new Complex-Network-based solution for determining the location of DESS without heavy computation from optimization tools. Compared to the node types, defined initially in complex networks, we propose a new bus type for reflecting the spatial operations of a storage element on the power grid. Then, a new metric ESP is defined with the comprehensive consideration of the structure and static factors that affect power grid operation. It integrates a new type storage bus and the structural net-ability features. The locations of DESSs can be selected by the ranked nodal ESP_n in descending order. This metric can determine the number and locations of DESS-affiliated buses. Meanwhile, a network-wide global metric ESP_G is also suggested for evaluating the network inherent ability in utilizing DESS. The simulation results in IEEE-30 with five different scenarios show that modification of the network structure has the most significant impacts on ESP_G . With higher ESP_G in different cases, the power grid's DESS utilization efficiency enforces, resulting in the equivalent 24-hour daily total cost decrement. Improvement of network performance by DESS depends on the original structure of the network and the relationship between supply and demand. Furthermore, a comparative evaluation between GA searching and ESP-GA hybrid searching is performed to assess all tested systems' computational efficiency and accuracy. The result indicates that the new hybrid search strategy is more time-effective than the GA siting and sizing search with less growth of the daily cost reduction rate. The result suggests that ESP can efficiently find quasi-optimal locations for ESS. Based on this work, we may expect that complex net-

ACKNOWLEDGMENT

This work was supported in part by the Research Development Fund (RDF-15-02-14 and RDF-18-01-04) of Xi'an Jiaotong-Liverpool University, and in part by the National Natural Science Foundation of China (51877181).

DATA AVAILABILITY STATEMENT

The data that support the findings of this study are available from the corresponding author upon reasonable request.

[1] N. Zhang, H. Jiang, Y. Li, P. Yong, M. Li, H. Zhu, S. G., and C. Kang, "Aggregating distributed energy storage: Cloud-based flexibility services from china," *IEEE Power Energy Mag.*, vol. 19, pp. 63–73, (2021).

[2] S.-X. Chen, H. B. Gooi, and M. Q. Wang, "Sizing of energy storage for microgrids," *IEEE Trans. Smart Grid*, vol. 3, pp. 142–151, (2012).

[3] F. Khatraei, R. Iravani, N. Hatzaegyiroti, and A. Dimeas, "Microgrids management," *IEEE Power Energy Mag.*, vol. 6, pp. 54–65, (2008).

[4] S. Vazquez, S. M. Lukic, E. Galvan, L. G. Franquelo, and J. M. Carrasco, "Energy storage systems for transport and grid applications," *IEEE Trans. Ind. Electron.*, vol. 57, pp. 3881–3895, (2010).

[5] M. J. O'Malley, M. B. Anwar, S. Heinen, T. Kober, J. McCalley, M. McPherson, M. Muratori, A. Ordis, M. Ruth, T. J. Schmidt, and A. Tuohy, "Multi-tier energy systems: Shaping our energy future," *Proceed. IEEE*, vol. 108, pp. 1437–1456, (2020).

[6] S. P. Burger, J. D. Jenkins, S. C. Huntington, and I. J. Perez-Arriaga, "Why distributed?: A critical review of the tradeoffs between centralized and decentralized resources," *IEEE Power Energy Mag.*, vol. 17, pp. 16–24, (2019).

[7] D. Hu, M. Ding, R. Bi, X. Liu, and X. Rong, "Sizing and placement of distributed generation and energy storage for a large-scale distribution network ESS. Based on this work, we may expect that complex net-

Planning of Distributed Energy Storage by A Complex Network Approach

766 work employing cluster partitioning," *J. Renew. Sustain. Energy* **10**, 025301 (2017).
 767 (2018). <https://doi.org/10.1063/1.5020246>.
 768 S. A. Bozorgavari, J. Aghaei, S. Prouzi, A. Nikoobakht, H. Farahmand, 801
 769 and M. Korpias, "Robust planning of distributed battery energy storage sys- 802
 770 tems in flexible smart distribution networks: A comprehensive study," *Re- 803
 771 new. Sust. Energ. Rev.* **123** (2020), 10.1016/j.rser.2020.109739.
 772 9 M. Hannan, M. Faisal, P. Jern Ker, R. Begum, Z. Dong, and C. Zhang, "Re- 805
 773 view of optimal methods and algorithms for sizing energy storage systems 806
 774 to achieve decarbonization in microgrid applications," *Renew. Sust. Energ.* 807
 775 **Rev.** **131**, 110022 (2020).
 776 10 J. H. Yi, R. Cherkasov, and M. Puelone, "Optimal allocation of ess in 810
 777 active distribution networks to achieve their dispatchability," *IEEE Trans.* 811
 778 **Power Syst.** **36**, 21068–2081 (2021).
 779 11 Y. M. Atwa and E. F. El-Saadany, "Optimal allocation of ess in distribution 812
 780 systems with a high penetration of wind energy," *IEEE Trans. Power Syst.* 813
 781 **25**, 1815–1822 (2010).
 782 12 G. Carpinelli, G. Celli, S. Mecci, F. Mattola, F. Pilo, and D. Proto, "Opti- 815
 783 mal integration of distributed energy storage devices in smart grids," *IEEE 816
 784 Trans. Smart Grid* **4**, 985–995 (2013).
 785 13 M. Sedghi, M. Aliakbar-Golkar, and M. R. Haghifam, "Distribution net- 817
 786 work expansion considering distributed generation and storage units using 818
 787 modified pso algorithm," *Int. J. Electr. Power Energy Syst.* **52**, 221–230 (2013).
 788 14 J. Liu, H. Cheng, Y. Tian, P. Zeng, and L. Yao, "Multi-objective bi-level 820
 789 planning of active distribution networks considering network transfer capa- 821
 790 bility and dispersed energy storage systems," *J. Renew. Sustain. Energy* **10**, 825
 791 015501 (2018), <https://doi.org/10.1063/1.4997511>.
 792 15 H. Pandzic, Y. S. Wang, T. Qiu, Y. Dvorkin, and D. S. Kirschen, "Near- 826
 793 optimal method for siting and sizing of distributed storage in a transmission 827
 794 network," *IEEE Trans. Power Syst.* **30**, 2288–2300 (2015).
 795 16 M. Ghorrani, A. Arabali, M. Etezadi-Amoli, and M. S. Fardali, "Energy 829
 796 storage application for performance enhancement of wind integration," 831
 797 *IEEE Trans. Power Syst.* **28**, 4803–4811 (2013).
 798 17 M. Zidar, P. S. Georgilakis, N. D. Hatziaerghiou, T. Capuder, and D. Skr- 832
 799 lec, "Review of energy storage allocation in power distribution networks: 833
 800 applications, methods and future research," *IET Gener. Transm. Distrib.* **10**, 836
 801 645–652 (2016).
 802 18 J. Y. Moon and J. Park, "Smart production scheduling with time-dependent 837
 803 resources and energy storage," *Int. J. Prod. Res.* **52**, 3922–3939 (2014).
 804 19 C. C. Chiu and H. H. C. Lu, "Complex networks theory for modern smart 839
 805 grid applications: A survey," *IEEE Trans. Emerg. Sel. Topics Circuits Syst.* 840

766 work employing cluster partitioning," *J. Renew. Sustain. Energy* **10**, 025301 (2017).
 767 (2018). <https://doi.org/10.1063/1.5020246>.
 768 S. A. Bozorgavari, J. Aghaei, S. Prouzi, A. Nikoobakht, H. Farahmand, 801
 769 and M. Korpias, "Robust planning of distributed battery energy storage sys- 802
 770 tems in flexible smart distribution networks: A comprehensive study," *Re- 803
 771 new. Sust. Energ. Rev.* **123** (2020), 10.1016/j.rser.2020.109739.
 772 9 M. Hannan, M. Faisal, P. Jern Ker, R. Begum, Z. Dong, and C. Zhang, "Re- 805
 773 view of optimal methods and algorithms for sizing energy storage systems 806
 774 to achieve decarbonization in microgrid applications," *Renew. Sust. Energ.* 807
 775 **Rev.** **131**, 110022 (2020).
 776 10 J. H. Yi, R. Cherkasov, and M. Puelone, "Optimal allocation of ess in 810
 777 active distribution networks to achieve their dispatchability," *IEEE Trans.* 811
 778 **Power Syst.** **36**, 21068–2081 (2021).
 779 11 Y. M. Atwa and E. F. El-Saadany, "Optimal allocation of ess in distribution 812
 780 systems with a high penetration of wind energy," *IEEE Trans. Power Syst.* 813
 781 **25**, 1815–1822 (2010).
 782 12 G. Carpinelli, G. Celli, S. Mecci, F. Mattola, F. Pilo, and D. Proto, "Opti- 815
 783 mal integration of distributed energy storage devices in smart grids," *IEEE 816
 784 Trans. Smart Grid* **4**, 985–995 (2013).
 785 13 M. Sedghi, M. Aliakbar-Golkar, and M. R. Haghifam, "Distribution net- 817
 786 work expansion considering distributed generation and storage units using 818
 787 modified pso algorithm," *Int. J. Electr. Power Energy Syst.* **52**, 221–230 (2013).
 788 14 J. Liu, H. Cheng, Y. Tian, P. Zeng, and L. Yao, "Multi-objective bi-level 820
 789 planning of active distribution networks considering network transfer capa- 821
 790 bility and dispersed energy storage systems," *J. Renew. Sustain. Energy* **10**, 825
 791 015501 (2018), <https://doi.org/10.1063/1.4997511>.
 792 15 H. Pandzic, Y. S. Wang, T. Qiu, Y. Dvorkin, and D. S. Kirschen, "Near- 826
 793 optimal method for siting and sizing of distributed storage in a transmission 827
 794 network," *IEEE Trans. Power Syst.* **30**, 2288–2300 (2015).
 795 16 M. Ghorrani, A. Arabali, M. Etezadi-Amoli, and M. S. Fardali, "Energy 829
 796 storage application for performance enhancement of wind integration," 831
 797 *IEEE Trans. Power Syst.* **28**, 4803–4811 (2013).
 798 17 M. Zidar, P. S. Georgilakis, N. D. Hatziaerghiou, T. Capuder, and D. Skr- 832
 799 lec, "Review of energy storage allocation in power distribution networks: 833
 800 applications, methods and future research," *IET Gener. Transm. Distrib.* **10**, 836
 801 645–652 (2016).
 802 18 J. Y. Moon and J. Park, "Smart production scheduling with time-dependent 837
 803 resources and energy storage," *Int. J. Prod. Res.* **52**, 3922–3939 (2014).
 804 19 C. C. Chiu and H. H. C. Lu, "Complex networks theory for modern smart 839
 805 grid applications: A survey," *IEEE Trans. Emerg. Sel. Topics Circuits Syst.* 840

20 E. Bompard, D. Wu, and F. Xue, "Structural vulnerability of power sys-
 tems: A topological approach," *Electr. Power Syst. Res.* **81**, 1334–1340
 (2011).
 21 S. W. Mei, F. He, X. M. Zhang, S. Y. Wu, and G. Wang, "An improved opa
 model and blackout risk assessment," *IEEE Trans. Power Syst.* **24**, 814–823
 (2009).
 22 E. Bompard, R. Napoli, and F. Xue, "Extended topological approach for
 the assessment of structural vulnerability in transmission networks," *IET
 Gener. Transm. Distrib.* **4**, 716–724 (2010).
 23 V. Latora and M. Marchiori, "Efficient behavior of small-world networks,"
Phys. Rev. Lett. **87** (2001).
 24 G. A. Pagnan and N. Aletro, "From the grid to the smart grid, topologically,"
Physica A **449**, 160–175 (2016).
 25 S. Aranas, E. Bompard, A. Carbone, and F. Xue, "Power grid vulner-
 ability: A complex network approach," *Chaos* **19** (2009), Artn 013119
 10.1063/1.3077229.
 26 E. Bompard, R. Napoli, and F. Xue, "Analysis of structural vulnerabilities
 in power transmission grids," *Int. J. Crit. Infrastruct. Prot.* **2**, 5–12 (2009).
 27 H. Ronellentisch, M. Timme, and D. Witthaut, "A dual method for com-
 puting power transfer distribution factors," *IEEE Trans. Power Syst.* **32**,
 1007–1015 (2017).
 28 M. Papadimitrakis, N. Giannarolis, M. Stogiannos, E. Zois, N.-I. Livanos,
 and A. Alexandridis, "Metaheuristic search in smart grid: A review with
 emphasis on planning, scheduling and power flow optimization applica-
 tions," *Renewable and Sustainable Energy Reviews* **145**, 111072 (2021).
 29 Sarjaya, A. B. Mulyawan, A. Setiawan, and A. Sudiarso, "Thermal unit
 commitment solution using genetic algorithm combined with the principle
 of tabu search and priority list method," in *2013 International Conference
 on Information Technology and Electrical Engineering (ICTEE)* (2013) pp.
 414–419.
 30 R. D. Zimmerman, C. E. Murillo-Sanchez, and R. J. Thomas, "Matpower:
 Steady-state operations, planning, and analysis tools for power systems re-
 search and education," *IEEE Trans. Power Syst.* **26**, 12–19 (2011).
 31 K. Zou, A. P. Agalgaonkar, K. M. Muttaqi, and S. Perera, "Distribution
 system planning with incorporating dg reactive capability and system un-
 certainties," *IEEE Trans. Sustain. Energy* **3**, 112–123 (2012).
 32 "IEEE reliability test system," *IEEE Trans. Power Appar. Syst.* **98**, 2047–
 2054 (1979).
 33 IEEE, "300 bus power flow test case," Available at http://labs.ece.uw.edu/ptwca/pt300/pg_cca300bus.htm (1995).

